Hindawi
Advances in Civil Engineering
Volume 2024, Article ID 9599807, 8 pages
https://doi.org/10.1155/2024/9599807

Research Article

Mechanical Properties and Hardening Mechanism of Magnesium Ammonium Phosphate Cements Modified by Fly Ash

Ran Hai, Jingyu Zhang, Junxia Liu, Cun Hui, and Fei Yang

School of Architectural Engineering, Zhongyuan University of Technology, Zhengzhou 450007, Henan, China

Correspondence should be addressed to Junxia Liu; liujunxia@zut.edu.cn

Received 19 July 2023; Revised 7 December 2023; Accepted 2 January 2024; Published 19 January 2024

Academic Editor: Robert Černý

High hydration heat and poor water resistance are the main factors restricting the application of magnesium ammonium phosphate cement (MAPC). To alleviate the problem, fly ash was used to partially replace dead-burned MgO and $NH_4H_2PO_4$ in this paper. The effect of fly ash content on MAPC properties, such as setting time, fluidity, mechanical properties, and water resistance, was investigated. The micromorphology of hydration products and the influence mechanism of fly ash on the macro-characteristics and hydration process of MAPC were also discussed. The results showed the mechanical properties of fly ash-modified MAPC decreased with the increase of the fly ash content, but their increments at later hydration were greater than the control MAPC. Meanwhile, fly ash could improve the water-resistance significantly and reduce the total hydration heat. The fly ash refined the struvite crystal and increased the compactness of MAPC, although no obvious hydration products of fly ash were observed. So, when the content of fly ash is 30 wt%, the MAPC has appropriate mechanical properties, while its water resistance is significantly improved, and its hydration heat is reduced compared with the control group.

1. Introduction

Magnesium phosphate cement (MPC) is a new type of inorganic cementitious material prepared with dead-burnt magnesia oxide (MgO), acid phosphates, and admixture in a specific ratio, which is achieved at room temperature through an acid–base chemical reaction and physical action [1]. Due to the high early strength, quick setting and hardening, and high bonding strength with preexisting concrete, MPC has received extensive attention in the field of the quick repair of building structures [2, 3].

At present, MPC and its repair mortar are mainly used for airport highways, military engineering, maritime engineering, urban traffic road pavement, and other key projects of short-term repair work. Owing to the high hydration temperature, concentrated heat release, poor water resistance, and high cost, the application and promotion of MPC are limited. However, mineral admixtures such as fly ash, slag, silica fume, and red mud can effectively overcome these problems through the pozzolanic activity and filling effect [4, 5].

Mineral admixtures not only improve the fluidity, later strength, water stability, and volume stability of MPC but also reduce the cost [6], among which considerable focus has been placed on research involving MPC modified by fly ash. Li et al. [7] demonstrated that incorporating fly ash could significantly increase the setting time of MPC. Based on the morphology effect of fly ash glass beads, the fluidity of MPC was increased, and the color of the hardened MPC could be adjusted [8, 9]. Incorporating an appropriate percent of fly ash could optimize the pore structure of MPC, improve the compaction, and subsequently increase the mechanical properties [10, 11]. According to Mao et al. [12], the compressive strength of magnesium ammonium phosphate cement (MAPC) cured in water for 28 days with 30% fly ash was equivalent to that of MAPC without fly ash cured under air curing conditions, which was consistent with the conclusion of the literature [13], indicating that fly ash could improve the water-resistance of MPC. Jiang et al. [14] tested the volume stability of MPC-hardened samples and discovered that fly ash can effectively reduce the number of microcracks.

Fly ash not only affects the macroperformance of MPC but also changes the hydration process, hydration products, and hydration heat control of MPC. It was reported that the addition of fly ash could lower the total hydration heat and

Table 1: Chemical composition of dead-burnt magnesia oxide and fly ash (wt%).

Raw materials	MgO	SiO_2	Al_2O_3	Fe_2O_3	CaO	K_2O	SO_3	TiO_2	P_2O_5
MgO	91.46	2.03	1.02	1.27	1.75	0.04	0.20	0.04	0.13
Fly ash	0.57	34.54	21.18	3.42	3.06	1.53	0.21	0.94	0.18

the peak hydration temperature of MPC [15]. Fly ash was ever considered to be an inert material that filled the MPC [16], but recent evidence suggests that fly ash can react within MPC systems. Xu et al. [11] used fly ash as an inert and reactive material in various formulation designs. It was found that fly ash particles were well encased by struvite, as shown by scanning electron microscopy (SEM), demonstrating the compatibility. Additionally, some fly ash hydration products could also be seen, although X-ray diffraction and thermogravimetric analysis failed to detect them. Gardner et al. [17] observed that the hydration products were rich in Si and Al through an nuclear magnetic resonance cross-polarization reaction, but the nature of the reaction products could not be established.

The aforementioned research demonstrates that the addition of fly ash can significantly increase the fluidity, compactness, and volume stability of MPC; nevertheless, the research on the effect mechanism still needs to be further developed. So, this paper focuses on the hydration process, water stability, and mechanical properties of MPC, as well as the composition and structure of the hydration products and their relationship to macroproperties. Based on previous research [18], this paper prepared MAPC by partially substituting dead-burnt MgO and $NH_4H_2PO_4$ with fly ash and investigated the effects of the fly ash content on the setting time, fluidity, mechanical properties, water resistance, and hydration heat of MAPC. SEM was used to study the hydration product composition, micromorphology, and hydration hardening process of MAPC, and the mechanism of the effect of fly ash on the macroscopic properties of MAPC was elucidated, which laid the foundation for realizing the engineering application of fly ash-modified MAPC.

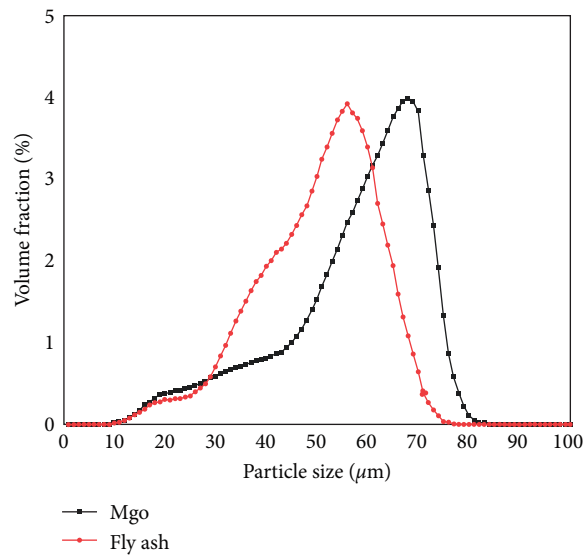

Figure 1: Particle size distribution of calcined magnesia and fly ash.

Table 2: Mixure of MAPC.

Mixture ID	M + P (wt%)	Fly ash (wt%)	M/P	W/B	N/M (wt%)
FA0	100	0	3/1	0.20	12
FA10	90	10	3/1	0.20	12
FA20	80	20	3/1	0.20	12
FA30	70	30	3/1	0.20	12
FA40	60	40	3/1	0.20	12
FA50	50	50	3/1	0.20	12

2. Materials and Methods

2.1. Materials. Dead burnt MgO was provided by Liaoning Tianyi Refractory Co., Ltd. China, which was produced by calcining magnesite under a temperature of 1,780°C; the specific surface area and average particle size measured by laser granularity analyzer were 764.0 m^2/kg and 28 μm respectively. The chemical composition is shown in Table 1, and the particle distribution is presented in Figure 1. The specific surface area of secondary fly ash used in the research was 393.5 m^2/kg, and the particle distribution is also presented in Figure 1. The chemical composition analyzed by X-ray fluorescence spectrometer is listed in Table 1. The purity of industrial grade $NH_4H_2PO_4$ provided by Sichuan Ronglv Technology Ltd exceeded 90%. The retarder adopted analytical pure $Na_2B_4O_7 \cdot 5H_2O$ was supplied by Shanghai Xinda Chemical Co., Ltd.

2.2. Mixture Proportion. Mix proportions of the MAPC are provided in Table 2, where M + P was for the sum of the mass of dead-burnt MgO and $NH_4H_2PO_4$, M/P was the mass ratio of them; N/M represented the mass ratio of borax to dead-burnt MgO; B was the total mass of cementitious materials. The fly ash replacements were 0, 10, 20, 30, 40, and 50 wt%, respectively, by weight of magnesia oxide and $NH_4H_2PO_4$. According to the fly ash replacement level, the mixtures are referred to as FA0, FA10, FA20, FA30, FA40, and FA50, respectively.

2.3. Experimental Methods

2.3.1. Physical and Mechanical Properties. According to Table 2, raw materials were weighed. First, MgO, $NH_4H_2PO_4$, fly ash, and borax were added into the mixer and stirred slowly for 30 s; subsequently, the weighed water was added to the mixer and stirred slowly for 30 s and then quickly for 60 s; finally, MAPC paste was obtained and quickly poured into the triple mold of 40 × 40 × 160 mm for vibration molding. The setting time and fluidity of MAPC were tested

according to GB/T 1346-2011 [19], taking the initial setting time as the setting time. The compressive strength and flexural strength were tested according to GB/T17671-2021, ISO [20].

The curing methods were divided into air curing and water curing. During air curing, the specimen was placed in the curing box, and the curing temperature was kept at 20°C, the relative humidity was between 50% and 70%. During water curing, the specimens were placed in the water tank of the curing room after 3 days of air curing. After the water-curing specimen reached the corresponding age, used a towel to wipe the surface moisture of the specimen and let it stand for 20 min. The water resistance of red mud MPC was measured according to Chinese standard GB/T 50082-2009 [21] and was quantitatively characterized with strength retention rate, which was the ratio in compressive strength of specimens cured in water for 28 days to those air curing for 28 days.

2.3.2. Hydration Heat. The hydration heat of fly ash MAPC was measured using a 12-channel microcalorimeter using the direct method (alternative method) in GB/T 12959-2008 [22]. Under constant temperature conditions, the calorimeter measured the temperature change caused by the hydration of MAPC and calculated the total heat accumulated and lost in the calorimeter, which in turn yields its heat of hydration. To avoid the steam pressure caused by the high peak temperature of hydration in the test process, the rubber plug with the thermometer of the thermos jar was pressed out, and the test process was affected. In this test, the total mass of fly ash-modified MAPC was 350 g, according to Table 2, the water at 20 ± 1°C was 300 g. The heat of cement was measured directly according to the calorimeter. Calculate the heat absorbed by the water using $Q = Cm\Delta t$ and added this heat to the heat measured by the calorimeter to obtain the cumulative heat release. Where C presented specific heat capacity, m presented quality, and Δt presented raised or lowered temperature.

2.3.3. Micromorphology and Mineral Composition of Hydration Products. After testing the strength of MAPC specimens at different ages, the broken pieces were collected and soaked in anhydrous ethanol for at least 7 days to stop hydration, and the specimens were dried in a vacuum drying oven at 60°C to constant weight before a microscopic test.

Before the SEM test, gold spraying was performed. The samples were subjected to a Quanta 250 FEG FE-SEM from an FEI company in the United States under the conditions of 3 kV accelerating voltage and three spot sizes. The micromorphology of fly ash particles, the changes in the interfacial transition zone between fly ash and paste, and the morphological characteristics of hydration products of MAPC at each age were observed.

3. Results and Discussion

3.1. Setting Time and Fluidity. Figure 2 shows that the setting time of MAPC decreases with increasing of fly ash content. When the content of fly ash is less than 40 wt%, the setting time shortens from 27 to 15 min. When the content of fly ash is 50 wt%, the setting time is slightly longer than that of FA40. This is because fly ash partially replaces MgO and $NH_4H_2PO_4$, which reduces the concentration of MgO and the retarder of the mixture, delays MgO dissolution and acid–base interaction, and ultimately shortens the setting time [23]. When the proportion of fly ash exceeds 40 wt%, the decreasing trend of the setting time is terminated under the combined action of the decrease of the concentration of H^+ dissociated from $NH_4H_2PO_4$ in the solution and the adsorption and encapsulation of fine fly ash particles.

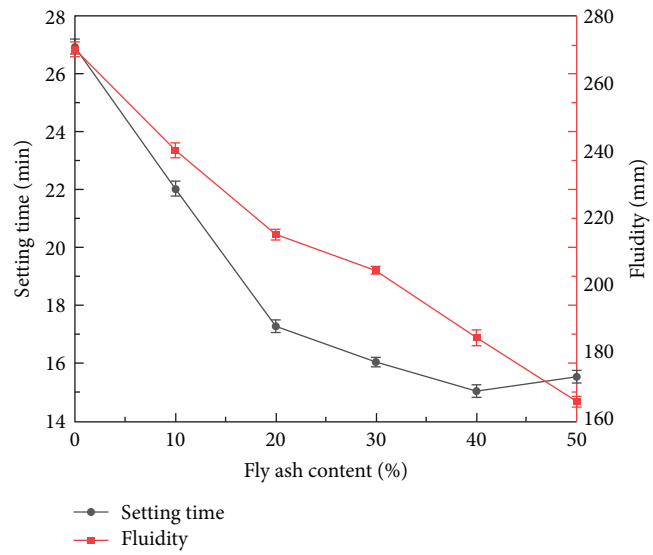

Figure 2: Setting time and fluidity of MAPC with different fly ash content.

It can be seen from Figure 2 that the fluidity of the MAPC mixture decreases with the increase of fly ash content. The fluidity reduces from 270 to 166 mm as fly ash content increases from 0 to 50 wt%. The particle size of fly ash is fine; therefore, the increase of the total surface area of MAPC raw materials leads to an increase in water demand, a decrease in the free water volume in the mixture, and a decrease in the fluidity.

3.2. Mechanical Properties. Figure 3(a) displays the effect of the fly ash contents on the compressive strength of MAPC. It is evident that the compressive strength of MAPC decreases with the increasing of fly ash content. When the fly ash content exceeds 10 wt%, the compressive strength of MAPC cured for 3 hr decreases the most, but the compressive strength at 3 and 28 days increase significantly. The increase in compressive strength of FA0 at 3 and 28 days is 14.8% and 29% higher than cured for 3 hr, respectively, while FA30 is 73.7% and 122.2%, which indicates that fly ash can significantly improve the later strength of MAPC. As can be seen from Figure 3(b) that the variation rule of flexural strength is similar to that of compressive strength, and both gradually decrease with the increase of fly ash content.

This is mainly because the content of $Mg(NH_4)PO_4{\cdot}6H_2O$, the main hydration product of MAPC, decreases with the increasing of replacement of fly ash, and its mechanical properties decrease accordingly. Meanwhile, the potential active components such as amorphous alumina and ferric

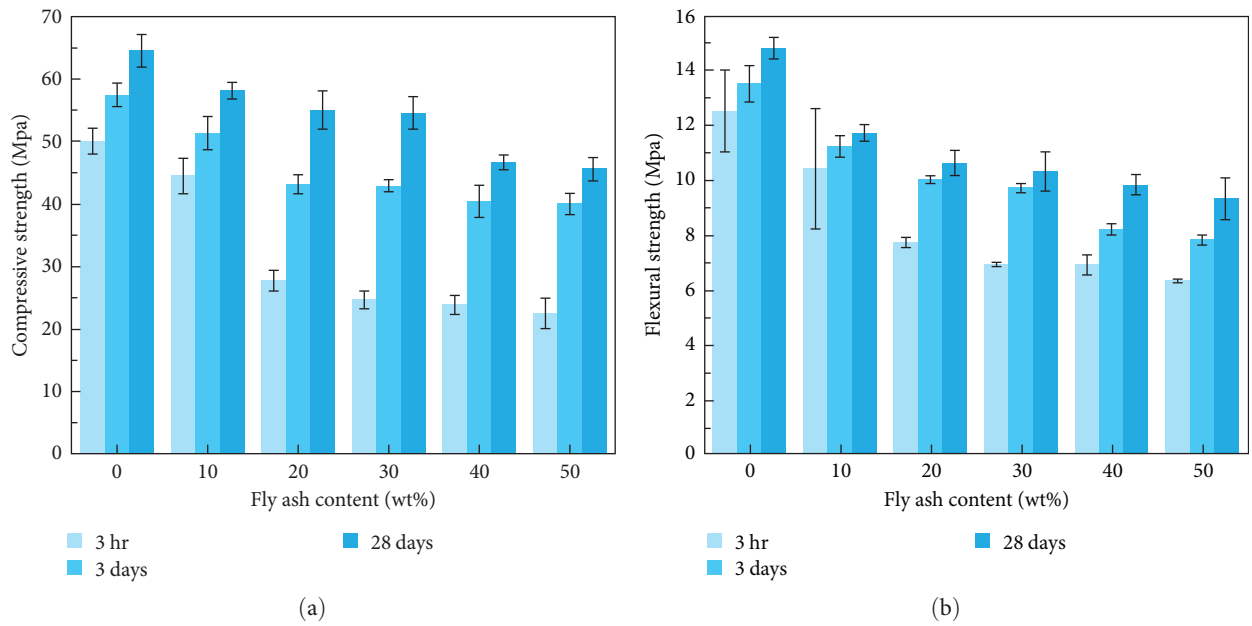

Figure 3: Mechanical properties of MAPC with different fly ash content: (a) compressive strength; (b) flexural strength.

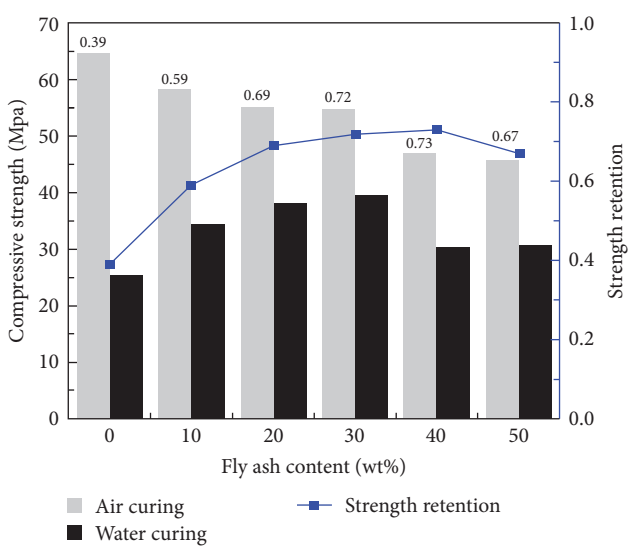

Figure 4: Water resistance of MAPC with different fly ash content.

oxide enriched in fly ash consume a few phosphate, which reduce the reaction between MgO and $NH_4H_2PO_4$ and the formation of the hydration product $Mg(NH_4)PO_4{\cdot}6H_2O$. Moreover, unburned carbon and other impurities of fly ash can adhere to the surface of the initial hydration product, creating a loose porous structure, thereby reducing the mechanical properties of MAPC [24]. Due to the pozzolanic effect of fly ash, the difference in the mechanical properties between fly ash-modified MAPC and FA0 is reduced at the later hydration stage [25]. So, when the content of fly ash is no more than 30 wt%, the compressive strength and flexural strength of MAPC cured for 28 days are still higher than 50 and 10 MPa, respectively.

3.3. Water Resistance. The strength retention ratio is an indicator of the water resistance of materials. As shown in Figure 4, when the content of fly ash is lower than 40 wt%, strength retention increases with the increase of the fly ash content and is up to 0.73; continue to increase the fly ash to 50 wt%, and the strength retention is decreased to 0.67, but still higher than the control group FA0; the results indicate that the addition of fly ash can improve the water-resistance of MAPC. The above results are mainly caused by the following two aspects: on the one hand, the addition of fly ash improves the microaggregate effect, reduces porosity, refines the pore structure, efficiently fills the micropores, and increases water stability [9]. On the other hand, as an amorphous silicon–aluminum material, the secondary hydration reaction of fly ash occurs at the later stage of hydration and increases with the increasing of the alkalinity of the cementitious materials system so as to refine the pore structure and improve the stability of MAPC [26]. When the content of fly ash is higher than 40 wt%, the amount of struvite in the hydration products of MAPC decreases, and so, the strength retention rate decreases.

3.4. Thermodynamic Analysis of Hydration Reaction. At the initial stage of hydration, $NH_4H_2PO_4$ is ionized and hydrolyzed to NH_4^+, $H_2PO_4^-$, HPO_4^{2-}, and H^+ according to thermodynamic Equations (1) and (2). At the second stage, MgO dissociates into Mg^{2+} and $[Mg(H_2O)]_6^{2+}$ in an acidic environment according to thermodynamic Equations (3) and (4), and then the acid–base neutralization reaction occurs to generate $Mg(NH_4)PO_4{\cdot}6H_2O$ according to the Equation (5). In the third stage, the formation and crystallization of struvite hinder the migration of water and H^+ in the solution and the hydration speed decreases.

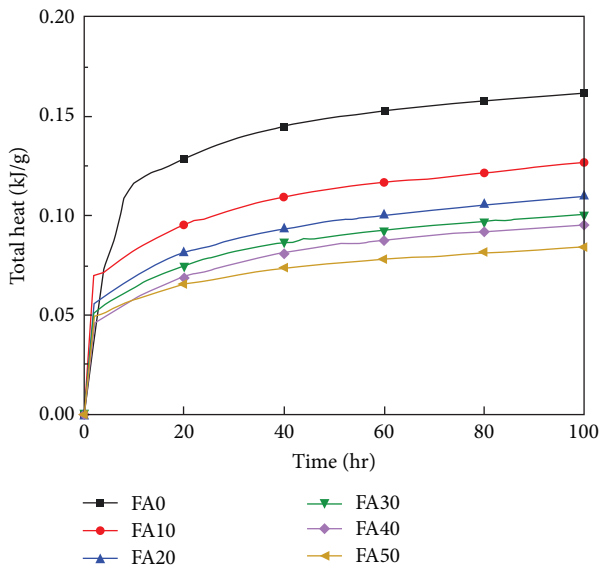

Figure 5: Hydration heat per powder mass of fly ash-modified MAPC hydrated 100 hr.

$$NH_4H_2PO_4 = NH_4^+ + H_2PO_4^- \ \Delta H = +19.7\,\text{kJ/mol}, \tag{1}$$

$$H_2PO_4^- = H^+ + HPO_4^{2-} \ -\Delta H = +4.2\,\text{kJ/mol}, \tag{2}$$

$$MgO + 2H^+ = Mg^{2+} + H_2O \ \Delta H = -151.1\,\text{kJ/mol}, \tag{3}$$

$$Mg^{2+} + 6H_2O = [Mg(H_2O)]6^{2+} \ \Delta H = +374.5\,\text{kJ/mol}, \tag{4}$$

$$[Mg(H_2O)6^{2+}] + HPO_4^{2-} + NH_4^+ \rightarrow Mg(NH_4)PO_4 \cdot 6H_2O + H^+ \ \Delta H = -449.3\,\text{kJ/mol}. \tag{5}$$

Figure 5 displays the hydration heat per powder mass of MAPC with various fly ash contents within 100 hr. As can be seen from Figure 5, FA0 per unit mass releases the highest hydration heat in the early stage, which is 0.12 kJ/g for 10 hr, reaching 75.0% of the cumulative hydration heat; those of FA10 are 0.08 kJ/g and 61.5%, respectively, while those of FA50 are only 0.05 kJ/g and 62.5%. Results indicate that fly ash can alleviate the centralized heat release problem of MAPC. The cumulative hydration heat of MAPC for 100 hr increases continuously with the hydration reaction and decreases with the increase in fly ash content.

The cumulative heat released in the hydration process of MAPC is calculated according to the hydration heat Equations (1)–(5) [27]. The measured and theoretical cumulative hydration heat calculated based on the mass and molar mass of MgO and $NH_4H_2PO_4$ participating in the hydration heat test is shown in Table 3. The measured values of the hydration heat of MAPC are all lower than the theoretical value, among which FA10, FA20, and FA30 have larger differences. Owing to the adsorption effect of fly ash on $NH_4H_2PO_4$, the H^+ content in the system and the amount of dissolved MgO decreases [28]; at the same time, a large amount of water evaporates during the hydration process, the degree of hydration reaction is not sufficient; in addition, fly ash has a very low self-hydration heat [29]. So, the cumulative hydration heat per powder mass released in 100 hr decreases gradually.

Table 3: The amount and cumulative heat per powder mass release of raw materials.

Mix ID	Mass (g)			Amount of substance (mol)			Hydration heat per powder mass (kJ/g)	
	M	P	H_2O	M	P	H_2O	Theoretical	Measured
FA0	203.5	67.8	54.3	5.05	0.59	3.01	0.18	0.16
FA10	184.4	61.5	54.3	4.58	0.53	3.01	0.16	0.13
FA20	165.1	55.0	54.3	4.10	0.48	3.01	0.14	0.11
FA30	145.5	48.5	54.3	3.61	0.42	3.01	0.12	0.10
FA40	125.6	41.9	54.3	3.12	0.36	3.01	0.11	0.10
FA50	101.7	33.9	54.3	2.52	0.29	3.01	0.09	0.08

3.5. SEM Analysis. Figure 6 represents the micromorphology of the control group MAPC cured for 3 hr, 3, and 28 days. Figure 6(a) reveals that there are a few irregular columnar crystals, microcracks, and micropores on the sample, indicating that the hydrated struvite has started to emerge after curing 3 hr and that the overall structure is not tightly connected. After 3 days of hydration, the columnar crystal progressively grows and becomes slightly compact, as shown in Figure 6(b). The SEM images of FA0 cured for 28 days (Figure 6(c)) demonstrate that struvite grows visibly and overlaps with each other. There is no obvious crack at the interface with MgO crystal, and the density of the hydration products is significantly increased.

Figure 7 characterizes the micromorphology of MAPC cured for 28 days with varying fly ash content. The section of fly ash-modified MAPC contains visible fly ash particles and glass beads. The struvite gradually declines as the content of fly ash increases. When the fly ash content is less than 30 wt%, the fly ash particles are evenly distributed between the closely bonded struvite and MgO, and the compactness of MAPC is improved to varying degrees, so its mechanical properties are not significantly reduced, and water resistance is gradually improved. The amount of fly ash keeps growing, the hydration products attached to the surfaces of fly ash particles significantly decrease, and the continuity of the struvite significantly diminishes, but the compactness is still higher than FA0. Therefore, the mechanical properties are reduced, and the water resistance is still significantly higher than that of FA0. In Figure 7(f), the unhydrated cylindrical dense MgO crystal can be observed. The acidity in the system decreases as the replacement amount of fly ash reaches 50 wt%, and the dissolving and hydration rate of MgO is lowered, so the mechanical characteristics of hardened MAPC are reduced.

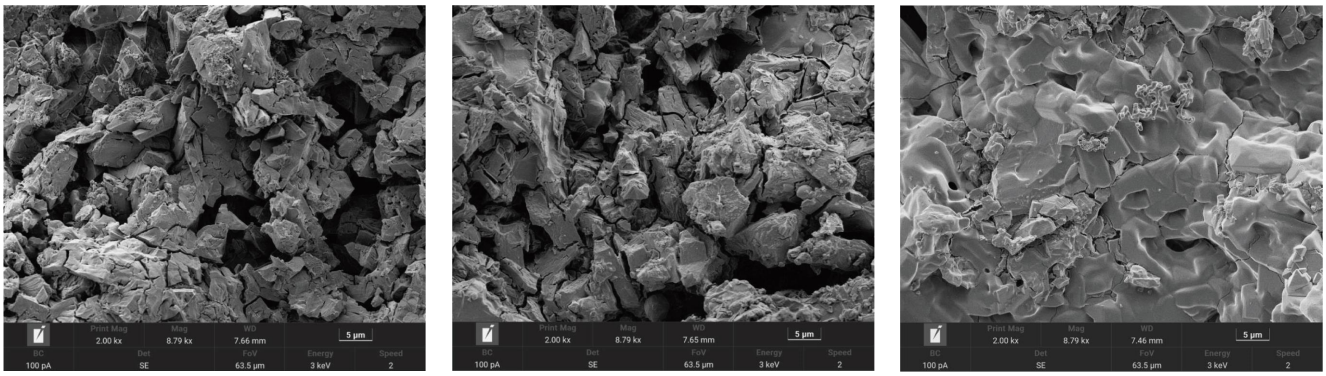

(a) (b) (c)

Figure 6: SEM images of FA0 at 3 hr, 3, and 28 days: (a) FA0 3 hr; (b) FA0 3 days; (c) FA0 28 days.

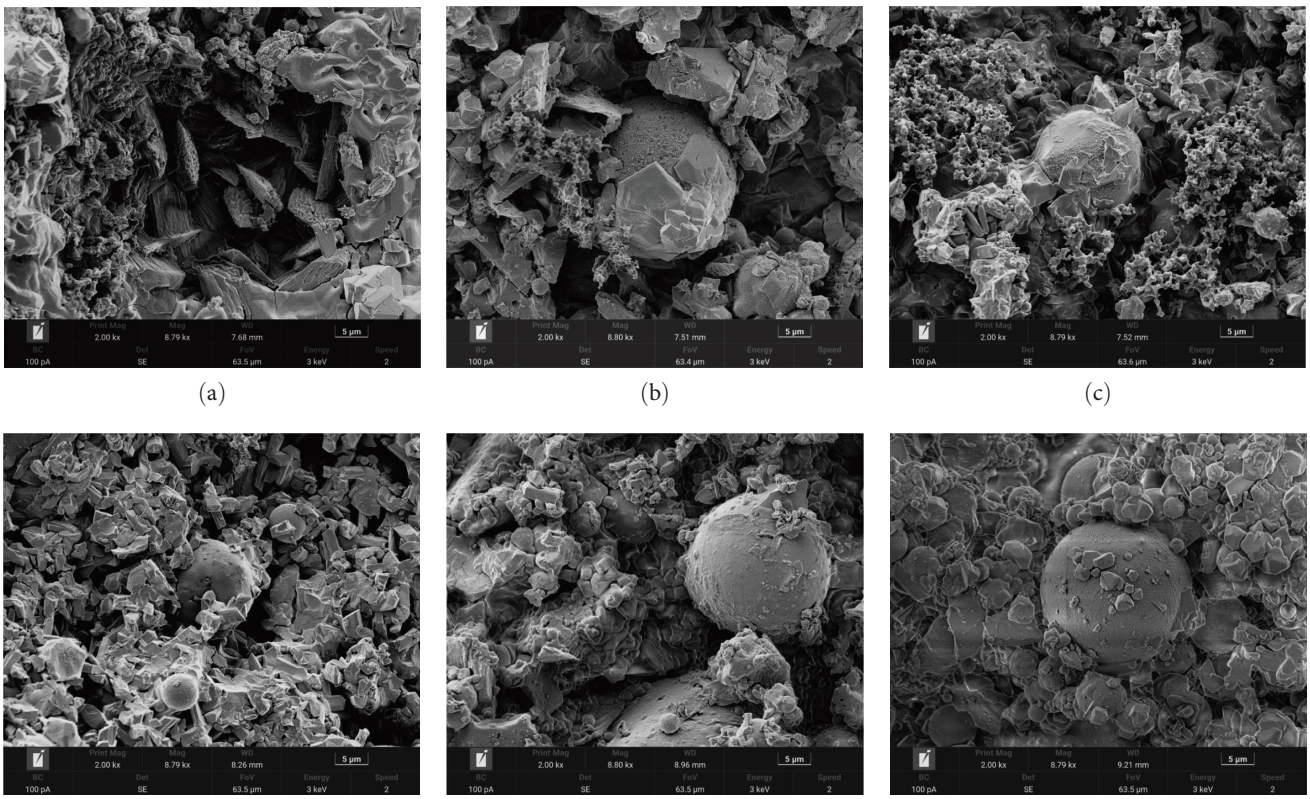

(a) (b) (c)

(d) (e) (f)

Figure 7: SEM images of fly ash-modified MAPC at 28 days: (a) FA0 28 days; (b) FA10 28 days; (c) FA20 28 days; (d) FA30 28 days; (e) FA40 28 days; (f) FA50 28 days.

4. Conclusions

This article mainly studied the variation of the fluidity, setting time, mechanical properties, and water resistance of MAPC with the amount of fly ash. The influence mechanism of fly ash on macroscopic properties was elucidated based on the composition and morphology analysis of hydration products. Additionally, the effect of fly ash on the hydration and hardening process of MAPC was clarified through the analysis of hydration heat and hydration reaction thermodynamics. According to the experimental results, the following conclusions were drawn:

(1) The setting time of fly ash-modified MAPC decreases first and then increases with the increase of fly ash content. The fluidity and mechanical properties of MAPC gradually decreased with the increase of fly ash content, but the increment in mechanical properties at the later hydration stage is greater than the control MAPC.

(2) The water resistance of fly ash-modified MAPC shows a trend of first increasing and then decreasing with the rising content of fly ash. When the fly ash content is 30 wt%, the compressive strength and flexural strength of MAPC cured for 28 days are still higher than 50 and 10 MPa, respectively, and its strength retention rate is 0.72, which is 1.85 times of the control group.

(3) Most of the hydration heat of MAPC is intensively released in 10 hr, and the total hydration heat and its increasing rate decrease with the increase of fly ash content. The measured value of accumulative hydration heat of MAPC within 100 hr is lower than the theoretical value.

(4) The main mineral compositions of MAPC at each age are unhydrated MgO and $Mg(NH_4)PO_4{\cdot}6H_2O$. The fly ash refines the struvite crystal and increases the compactness of MAPC, so its water resistance is improved. Meanwhile, with the increasing of fly ash content, the crystallinity and continuity of struvite decrease, which leads to a decrease in its mechanical properties.

5. Future Work

Future work will focus on research on the setting, hardening mechanism, and water resistance of fly ash-modified magnesium ammonium phosphate mortars under negative temperatures.

Data Availability

All datasets generated during this study are available from the corresponding author upon reasonable request.

Conflicts of Interest

The authors declare that they have no conflicts of interest.

Acknowledgments

This work was supported by the Henan Provincial Science and Technology tackling projects, grant no. 232102230132.

References

[1] T. Li, G. Chen, J. Yang, L. Chong, and X. Hu, "Influence of curing conditions on mechanical properties and microstructure of magnesium potassium phosphate cement," *Case Studies in Construction Materials*, vol. 17, Article ID e01264, 2022.

[2] B. Xu, F. Winnefeld, J. Kaufmann, and B. Lothenbach, "Influence of magnesium-to-phosphate ratio and water-to-cement ratio on hydration and properties of magnesium potassium phosphate cements," *Cement and Concrete Research*, vol. 123, Article ID 105781, 2019.

[3] L. Zhang, A. Zhang, Q. Wang et al., "Corrosion resistance of wollastonite modified magnesium phosphate cement paste exposed to freeze–thaw cycles and acid–base corrosion," *Case Studies in Construction Materials*, vol. 13, Article ID e00421, 2020.

[4] M. A. Haque and B. Chen, "Research progresses on magnesium phosphate cement: a review," *Construction and Building Materials*, vol. 211, pp. 885–898, 2019.

[5] H. Ma and Y. Li, "Discussion of the paper "characterisation of magnesium potassium phosphate cement blended with fly ash and ground granulated blast furnace slag" by L.J. Gardner et al." *Cement and Concrete Research*, vol. 103, pp. 245–248, 2018.

[6] Q. Fang, B. Xiao, Y. Chen, and Z. Ding, "Review on research progress of mineral admixtures in magnesium phosphate cement," *Concrete*, vol. 06, pp. 67–72, (in Chinese), 2021.

[7] J. Li, W. Zhang, and Y. Cao, "Laboratory evaluation of magnesium phosphate cement paste and mortar for rapid repair of cement concrete pavement," *Construction and Building Materials*, vol. 58, pp. 122–128, 2014.

[8] Q. Yang, S. Zhang, and X. Wu, "Deicer-scaling resistance of phosphate cement-based binder for rapid repair of concrete," *Cement and Concrete Research*, vol. 32, no. 1, pp. 165–168, 2002.

[9] Y. Li and B. Chen, "Factors that affect the properties of magnesium phosphate cement," *Construction and Building Materials*, vol. 47, pp. 977–983, 2013.

[10] Z. Ding and Z. Li, "High-early-strength magnesium phosphate cement with fly ash," *ACI Materials Journal*, vol. 102, no. 6, pp. 375–381, 2005.

[11] B. Xu, H. Ma, H. Shao, Z. Li, and B. Lothenbach, "Influence of fly ash on compressive strength and micro-characteristics of magnesium potassium phosphate cement mortars," *Cement and Concrete Research*, vol. 99, pp. 86–94, 2017.

[12] M. Mao, Z. Wang, and X. Jia, "Researching on water resistance improvement of magnesium phosphate cement," *Non-Metallic Mines*, vol. 35, pp. 1–3, (in Chinese), 2012.

[13] Y. Huang, J. Qian, Q. Wang, L. Su, Z. Lai, and C. You, "Influence of fly ash on water resistance of magnesia phosphate cement," *Materials Review*, vol. 25, pp. 470–473, (in Chinese), 2011.

[14] Z. Jiang, C. Qian, and Q. Chen, "Experimental investigation on the volume stability of magnesium phosphate cement with different types of mineral admixtures," *Construction and Building Materials*, vol. 157, pp. 10–17, 2017.

[15] L. J. Gardner, S. A. Bernal, S. A. Walling, C. L. Corkhill, J. L. Provis, and N. C. Hyatt, "Response to the discussion by Hongyan Ma and Ying Li of the paper "characterization of magnesium potassium phosphate cement blended with fly ash and ground granulated blast furnace slag"," *Cement and Concrete Research*, vol. 103, pp. 249–253, 2018.

[16] D.-D. Zheng, T. Ji, C.-Q. Wang, C.-J. Sun, X.-J. Lin, and K. M. A. Hossain, "Effect of the combination of fly ash and silica fume on water resistance of magnesium–potassium phosphate cement," *Construction and Building Materials*, vol. 106, pp. 415–421, 2016.

[17] L. J. Gardner, S. A. Bernal, S. A. Walling, C. L. Corkhill, J. L. Provis, and N. C. Hyatt, "Characterisation of magnesium potassium phosphate cements blended with fly ash and ground granulated blast furnace slag," *Cement and Concrete Research*, vol. 74, pp. 78–87, 2015.

[18] J. Liu, Z. Li, M. Zhang, and R. Hai, "A review of magnesium phosphate cement modified by mineral admixtures," *Inorganic Chemistry: An Indian Journal*, vol. 54, pp. 18–23, (in Chinese), 2022.

[19] GB/T 1346-2011, "Test methods for water requirement of normal consistency, setting time and soundness of the portland cement," Standards Press of China, Beijing, 2011.

[20] GB/T 17671-2021, "Test method of cement mortar strength (ISO method)," Standards Press of China, Beijing, 2021.
[21] GB/T 50082-2009, "Standard for test methods of long-term performance and durability of ordinary concrete," Standards Press of China, Beijing, 2009.
[22] GB/T 12959-2008, "Test methods for heat of hydration of cement," Standards Press of China, Beijing, 2008.
[23] J. Liu, M. Yuan, R. Hai, F. Yang, J. Zhang, and A. Li, "Investigation of the mechanical physical properties of fly ash modified magnesium phosphate cement repair mortar cured at varying temperatures," *Buildings*, vol. 13, no. 1, Article ID 88, 2023.
[24] R. C. Joshi and V. M. Malhotra, "Relationship between pozzolanic activity and chemical and physical characteristics of selected Canadian fly ashes," *MRS Proceedings*, vol. 65, pp. 167–170, 1985.
[25] M. R. Ahmad, B. Chen, and J. Yu, "A comprehensive study of basalt fiber reinforced magnesium phosphate cement incorporating ultrafine fly ash," *Composites Part B: Engineering*, vol. 168, pp. 204–217, 2019.
[26] D. X. Li and C. H. Feng, "Study on modification of the magnesium phosphate cement-based material by fly ash," *Advanced Materials Research*, vol. 150-151, pp. 1655–1661, 2010.
[27] J. Liu, Y. Yan, Z. Li, F. Yang, R. Hai, and M. Yuan, "Investigation on the potassium magnesium phosphate cement modified by pretreated red mud: basic properties, water resistance and hydration heat," *Construction and Building Materials*, vol. 368, Article ID 130456, 2023.
[28] F. Hu, S. Nie, A. Guo, L. Lv, L. Chu, and J. Yu, "Fresh properties and compressive strength of MPC-based materials with blended mineral admixtures," *Case Studies in Construction Materials*, vol. 17, Article ID e01201, 2022.
[29] P. Frantzis and R. Baggott, "Transition points in steel fibre pull-out tests from magnesium phosphate and accelerated calcium aluminate binders," *Cement and Concrete Composites*, vol. 25, no. 1, pp. 11–17, 2003.